Synthesis of Iron(II) Octachlorotetrapyrazinoporphyrazine, Molecular Structure and Optical Properties of the (X⁻)₂FeTPyzPACl₈ Dianions with Two Axial Anionic Ligands (X⁻ = CN⁻, Cl⁻)

Ksenya A. Ustimenko,[a,b] Dmitri V. Konarev,[a@] Salavat S. Khasanov,[c] and Rimma N. Lyubovskaya[a]

[a]*Institute of Problems of Chemical Physics RAS, 142432 Chernogolovka, Russia*
[b]*Moscow State University, 119991 Moscow, Russia*
[c]*Institute of Solid State Physics RAS, 142432 Chernogolovka, Russia*
[@]*Corresponding author E-mail: konarev@icp.ac.ru*

Iron(II) octachlorotetrapyrazinoporphyrazine (FeTPyzPACl₈, 1) was obtained by a direct tetramerization reaction of 1,2-dichloro-4,5-dicyanopyrazine and iron(II) acetylacetonate in 1-chloronaphthalene at 220 °C. It was dissolved in o-dichlorobenzene by a complex formation reaction with the CN⁻ anions by adding bis(triphenylphosphoranylidene) ammonium cyanide (PPNCN). Salt (PPN⁺)₂{(CN⁻)₁.₇₄(Cl⁻)₀.₂₆FeTPyzPACl₈}·2C₆H₄Cl₂ (2) was obtained as single crystals by slow diffusion of hexane into the o-dichlorobenzene solution. It contains the {(CN⁻)₂(FeTPyzPACl₈)} dianions (74 %) together with mixed {(FeTPyzPACl₈)(CN⁻)(Cl⁻)} dianions (26 %). The conformation of tetrapyrazinoporphyrazine macrocycle in 2 was determined by single crystal X-ray analysis. Central 24-atom PA macrocycle is nearly planar but dichloropyrazine groups noticeably deviate relatively the mean 24-atom plane or are twisted. The iron(II) atoms are located exactly in the PA plane, the average equatorial Fe–N(PA) bond length is 1.941(3) Å and the axial Fe–C(C≡N) bond length is 1.962(6) Å. The position of Q- and Soret bands in the spectrum of 1 is at 656, 475 and 327 nm. The addition of two axial anionic ligands provides a greater number of bands in the visible range observed at 657, 550, 438, 415 and 326 nm.

Keywords: Iron(II) tetrapyrazinoporphyrazines, dianions, synthesis, molecular structure.

Синтез октахлортетрапиразинопорфиразина железа(II), молекулярная структура и оптические свойства дианионов (X⁻)₂FeTPyzPACl₈ с двумя аксиальными анионными лигандами (X⁻ = CN⁻, Cl⁻)

К. А. Устименко,[a,b] Д. В. Конарев,[a@] С. С. Хасанов,[c] Р. Н. Любовская[a]

[a]*Институт проблем химической физики РАН, 142432 Черноголовка, Россия*
[b]*Московский государственный университет, 119991 Москва, Россия*
[c]*Институт физики твердого тела РАН, 142432 Черноголовка, Россия*
[@]*E-mail: konarev@icp.ac.ru*

Октахлортетрапиразинопорфиразин железа(II), (FeTPyzPACl₈, 1) был получен прямой реакцией тетрамеризации 1,2-дихлор-4,5-дицианопиразина и ацетилацетонато железа(II) в 1-хлорнафталине при 220 °C. Полученное соединение было растворено в о-дихлорбензоле посредством реакции комплексообразования с CN⁻ анионами добавлением цианида бис(трифенилфосфоранилиден)аммония (PPNCN). Соль (PPN⁺)₂{(CN⁻)₁.₇₄ (Cl⁻)₀.₂₆FeTPyzPA Cl₈}·2C₆H₄Cl₂ (2) была получена в виде монокристаллов медленной диффузией гексана в дихлорбензольный раствор. Соединение содержит дианионы {(CN⁻)₂FeTPyzPACl₈} (74 %) вместе со смешанными дианионами {(CN⁻)(Cl⁻)FeTPyzPACl₈} (26 %). Конформация тетрапиразинпорфиразинового макроцикла в

Iron(II) Octachlorotetrapyrazinoporphyrazine Dianions

2 была определена по данным рентгено-структурного анализа на монокристалле. Центральный макроцикл, состоящий из 24 атомов, практически планарен, но дихлорпиразиновые группы значительно отклоняются относительно плоскости 24-атомов центрального макроцикла или повернуты относительно нее. Атомы железа находятся точно в плоскости порфиразина, средняя длина экваториальных связей Fe–N(PA) составляет 1.941(3) Å, а аксиальных связей Fe–C(C≡N) - 1.962(6) Å. Положение Q-полос и полосы Core в спектре *1* - при 656, 475 и 327 нм. Добавление двух аксиальных анионных лигандов увеличивает число полос поглощения в видимой области, которые наблюдаются при 657, 550, 438, 415 и 326 нм.

Ключевые слова: Железо(II) тетрапиразинопорфиразины, дианионы, синтез, молекулярная структура.

Introduction

Phthalocyanines are stable macrocyclic ligands that form complexes with a variety of metals. Metal complexes of phthalocyanines are well-known dyes due to they have very strong absorption in the visible region, high chemical and thermal stability. These molecules can also be used as active layers for solar cells, CD-R, LEDs, transistors, photoconductors, electrochromic displays and sensors. [1-4] Some metal phthalocyanines manifest catalytic and photocatalytic properties.[5] They can also be used as models of different photophysical processes.[6]

Metal phthalocyanines as donors can be oxidized by relatively weak oxidants, for example, iodine, to form radical cation compounds possessing semiconducting or quasi-one-dimensional metallic conductivity (in some cases down to 4 K).[7,8] Compounds with ferromagnetic properties were obtained based on tetracyanoethylene and manganese phthalocyanine or substituted naphthalocyanine.[9,10]

Compounds based on phthalocyanine anions can also demonstrate promising conducting and magnetic properties. Theoretical works predict metallic conductivity and superconductivity in the electron doped non-transition metal phthalocyanines.[11] The compound containing chains of alternating iron(I) phthalocyanine anions and decamethylchromocene cations, $\{Fe^IPc]^-\}\{(Cp^*_2Cr^{III})^+\}\cdot(C_6H_4Cl_2)_4$, exhibits ferrimagnetic properties.[12] Now the salts with negatively charged cobalt(I), iron(I) and metal free phthalocyanines and porphyrazines have been obtained. [13-19] However, anionic phthalocyanines with tetra-coordinated metal atoms are not deeply investigated so far because of weak acceptor properties of metal phthalocyanine and as a result high air sensitivity of their anions. Metal-free phthalocyanines are reduced with potential more negative than -0.6 V, whereas zinc(II), copper(II), nickel(II) and manganese(II) phthalocyanines are reduced with potential -0.8 ÷ -0.9 V.[20]

To increase the acceptor ability of metal macroheterocycles electron-withdrawing substituents such as Cl, F or CN can be attached to the phthalocyanine macrocycle or the number of nitrogen atoms in the macrocycle should be increased. For example, reduction potentials of copper(II) octacyanophthalocyanine, copper(II) tetrapyrazinoporphyrazine and copper(II) octacyanotetrapyrazinoporphyrazine are positively shifted by 0.15, 0.28 and 0.42 V relatively to copper(II) phthalocyanine.[21] Thus, namely metal(II) tetrapyrazinoporphyrazines containing sixteen nitrogen atoms in the macrocycle and electron-withdrawing substituents at the periphery of the molecule are quite promising to develop new acceptor components.

Now various methods for preparing substituted tetrapyrazinoporphyrazines with different donor substituents were developed.[22-27] Electron-withdrawing substituents such as cyano-, sulfophenyl-, 2-pyridyl and 2-(*N*-methyl)-pyridiniumyl are used to increase the acceptor ability of tetrapyrazinoporphyrazines.[21,28-31] Molecular structure of pyridine substituted tetrapyrazinoporphyrazine is determined by single-crystal X-ray analysis for cobalt(II) tetrakis[5,6-di(2-pyridyl)-2,3-pyrazino}porphyrazine, $Co^{II}TPyzPAPy_8$.[15] Substituted tetrapyrazinoporphyrazines are used in cancer and photodynamic therapy,[32-34] as components for capacitors,[35] and their nonlinear properties are analyzed.[29]

In this work we developed a simple method to synthesize iron(II) octachlorotetrapyrazinoporphyrazine, $FeTPyzPACl_8$ (**1**), bearing eight electron-withdrawing chlorine substituents attached to the electron deficient tetrapyrazinoporphyrazine macrocycle. We found the way to dissolve this porphyrazine by a complex formation reaction with the CN⁻ ligands and prepare single crystals of $(PPN^+)_2$ $\{(CN^-)_{1.74}(Cl^-)_{0.26}FeTPyzPACl_8\}\cdot 2C_6H_4Cl_2$ (2), where PPN^+ is the bis(triphenylphosphoranylidene)ammonium cation. That allows us to study the optical properties of $FeTPyzPACl_8$ as well as molecular structure and optical properties of corresponding $(X^-)_2FeTPyzPACl_8$ dianions containing two axial anionic ligands ($X = CN^-$, Cl^-).
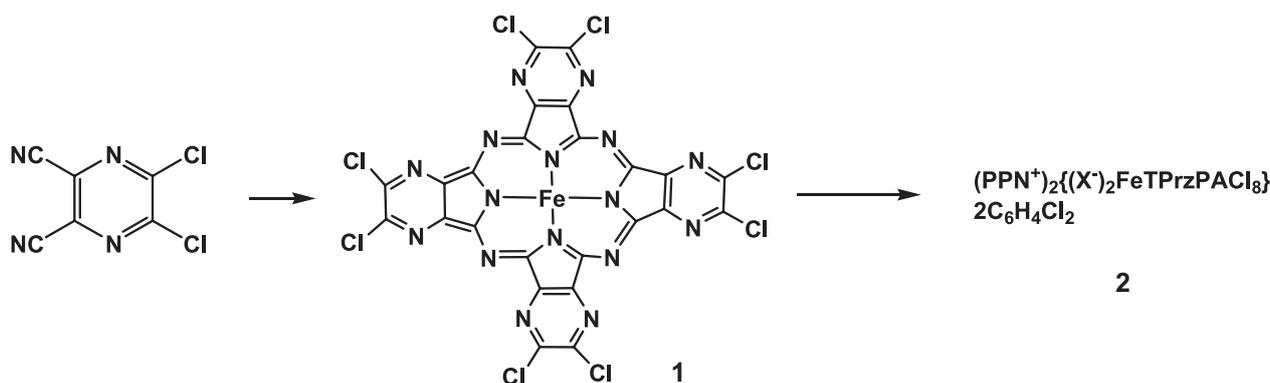
Experimental

General

UV-visible-NIR spectra were measured in KBr pellets on a Perkin Elmer Lambda 1050 spectrometer in the 250-2500 nm range. IR-spectra were measured in KBr pellets with a Perkin Elmer Spectrum 400 spectrometer (400-7800 cm⁻¹). Energy Dispersive X-ray analysis (EDX) was done with three crystals of **2** with SUPRA-50UP using electron microscope to obtain the Fe : P : Cl ratio.

Materials

1,2-Dichloro-4,5-dicyanopyrazine (TCI, 98 %), bis(triphenyl-phosphoranylidene)ammonium chloride (PPNCl, Aldrich, 99 %), iron(II) acetylacetonate (Aldrich, 99.95 %) and 1-chloronaphthalene (Aldrich, technical grade) were purchased. Solvents were purified in argon atmosphere. *o*-Dichlorobenzene ($C_6H_4Cl_2$) was distilled over CaH_2 under reduced pressure; hexane was distilled over Na/benzophenone. The solvents were degassed and stored in a glove box. Synthesis of **2** was carried out in a MBraun 150B-G glove box in controlled atmosphere with water and oxygen contents less than 1 ppm.

$(PPN^+)_2\{(X^-)_2FeTPrzPACl_8\}$
$2C_6H_4Cl_2$

2

1

Synthesis

Bis(triphenylphosphoranylidene)ammonium cyanide (PPNCN). 340 mg of NaCN was dissolved in 30 ml of absolute methanol (distilled over Mg turnings) and 2 g of PPNCl was added. After four hours of stirring at room temperature white precipitate of NaCl is formed which was filtered off. Obtained solution was evaporated to dryness with a rotary evaporator and white residue was dissolved in 30 ml of dry acetonitrile (distilled over CaH₂ under argon). Undissolved NaCN was filtered off and clear colorless solution was evaporated to dryness with a rotary evaporator to give white-yellowish crystalline PPNCN with 80 % yield. The hydroscopic solid was stored in the glove box.

Iron(II) octachlorotetrapyrazinoporphyrazine, FeTPyzPACl₈ (1). 1,2-Dichloro-4,5-dicyanopyrazine (1.2 g, 6 mmol) and iron(II) acetylacetonate (400 mg, 1.5 mmol) were heated at 220 °C on oil bath in 1-chloronaphthalene (14 ml) under argon upon intense stirring for 1 h. Reaction mixture turns green and black precipitate was formed. The solution was cooled down to room temperature and hexane (14 ml) was added to precipitate a black powder. Powder was filtered off and washed by two portion of acetone (100 ml and 50 ml). The obtained porphyrazine was transferred to a flask (50 ml) and washed with hot *o*-dichlorobenzene (20 ml) at 160 °C. The hot solution was filtered, and the obtained insoluble powder was washed with cold acetone (50 ml) and dried in vacuum for 2 h to yield 1.0 g (77 %). IR (KBr) ν cm⁻¹: main bands at 1260, 1195, 989, 787 and 697. UV-vis (KBr) λ nm: 327, 475 and 656.

The composition of obtained powder was determined by elemental analysis. It showed that additionally to porphyrazine **1** can also contain acetylacetone (C₅H₈O₂) and acetone (C₃H₆O). Found, %: C, 40.88; H, 1.82; N, 17.65; Cl, 23.60. Calculated, %: C, 41.60; H, 2.34; N, 18.71; Cl, 23.72. C₂₄N₁₆Cl₈Fe·2C₅H₈O₂·2.5C₃H₆O, M = 1197.

Preparation of (PPN⁺)₂{(CN⁻)₁.₇₄(Cl⁻)₀.₂₆FeTPyzPACl₈}· 2C₆H₄Cl₂ (2) as crystals. FeTPyzPACl₈ did not dissolve in *o*-dichlorobenzene even at 160 °C. However, when FeTPyzPACl₈ (40 mg) and 2.2 molar equivalents of PPNCN (58 mg) are stirred in *o*-dichlorobenzene (20 ml) at room temperature in the glove box for 24 h, it dissolved, and small amount of undissolved black powder is only remained. The solution was filtered in a 50 ml glass tube of 1.8 cm diameter with a ground glass plug, and 30 ml of hexane was layered over solution. Diffusion was carried out during one month. As a result 23 mg of black rhombic crystals were obtained with 22 % yields. Composition of the crystals was determined from X-ray diffraction on a single crystal and was confirmed by Energy Dispersive X-ray analysis (EDX) for three single crystals. Average observed Fe: P: Cl ratio for three crystals is 1: 4.1: 14.2, whereas the calculated data: Fe: P: Cl = 1: 4: 12.26. IR (KBr) ν cm⁻¹: main bands at 2103 (C≡N), 1260, 1193, 984, 782, 749, 692 and 501. UV-vis (KBr) λ nm: 326, 415, 438, 550 and 657.

X-Ray Crystal Structure Determination

Crystal data of **2**: $C_{109.74}H_{68}Cl_{12.26}FeN_{19.74}P_4$, M_r = 2277.43 g·mol⁻¹, black plate, triclinic, a = 12.0292(3), b = 14.9546(4), c = 16.2794(5) Å, α = 110.0160(10)°, β = 106.1290(10)°, γ = 98.8010(10)°, V = 2541.52(12) Å³, Z = 1, d_{calc} = 1.488 g·cm⁻³, μ = 0.595 mm⁻¹, $F(000)$ = 1159, T = 150(2) K, max. $2\theta_{max}$ = 58.34°, reflections measured 23224, unique reflections 12155, R_{int} = 0.0348, reflections with $I > 2\sigma(I)$ = 7639, parameters refined 712, restraints 29, R_1 = 0.0550, wR_2 = 0.1725, G.O.F. = 1.008. CCDC number is 964849.

The intensity data for **2** at 150(2) K were collected on a Bruker Smart Apex II CCD with graphite monochromated MoK$_\alpha$ radiation using a Japan Thermal Engineering Co. cooling system DX-CS190LD. Raw data reduction to F^2 was carried out using Bruker SAINT.[36] The structure was solved by direct method and refined by the full-matrix least-squares method against F^2 using SHELX-97.[37] Non-hydrogen atoms were refined in the anisotropic approximation. Positions of hydrogen atoms were calculated geometrically. Subsequently, the positions of H atoms were refined by the "riding" model with U$_{iso}$ = 1.2U$_{eq}$ of the connected non-hydrogen atom.

Results and Discussion

Synthesis

A conventional synthetic method for preparing metal tetrapyrazineporphyrazine is the heating of substituted pyrazine-2,3-dicarbonitrile in high-boiling solvent (tri-chlorobenzene, dichlorobenzene or quinolone, *b.p.* >200 °C) with metal salt (anhydrous chloride or acetate) or free metal with addition of catalytic quantities of urea or ammonium molybdate.[25,26,34] We use commercially available 1,2-dichloro-4,5-dicyanopyrazine from TCI. Synthetic proce-dure was modified using 1-chloronaphthalene as solvent and iron(II) acetylacetonate as a source of iron. The reaction was carried out at 220 °C in argon atmosphere during 1 hour. FeTPyzPACl₈ (**1**) was washed with acetone and hot *o*-dichlorobenzene. Composition of compound **1** was determined by elemental analysis which showed a large amount of solvent molecules in the sample (acetylacetone and acetone). This supposition is supported by the IR-spectrum of **1** since additional bands are observed in the spectrum of **1** at 1550-1690 cm⁻¹ which can be attributed to the C=O stretching modes of acetylacetone and acetone (see Supporting information). These bands were not observed when compound **2** was obtained, which according to the X-ray diffraction data was acetylacetone
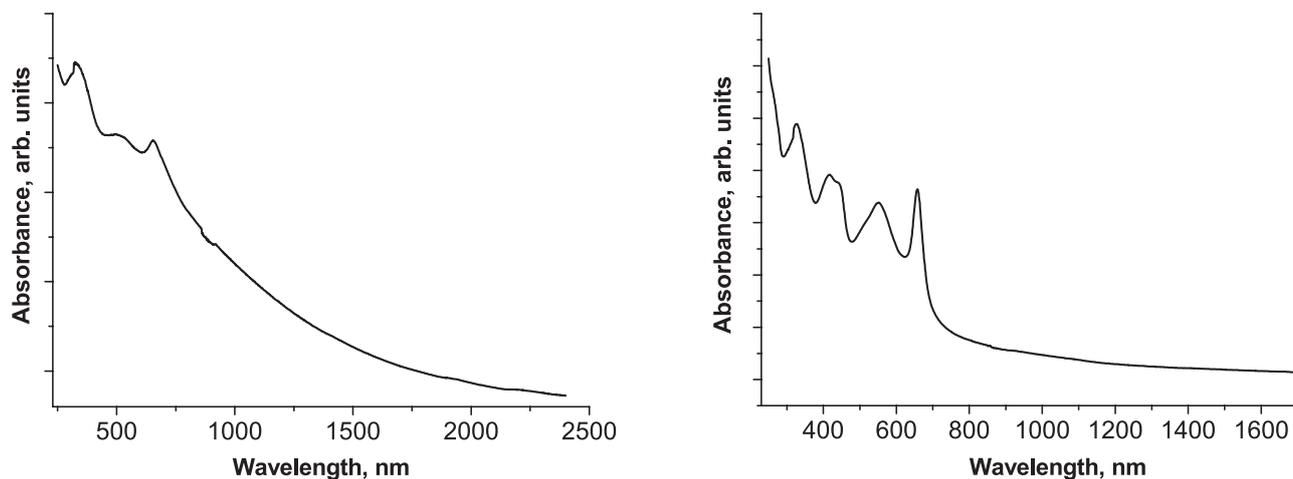
Figure 1. The UV-visible-NIR spectra of: (a) FeTPyzPACl$_8$ (**1**) in the 260-2400 nm range and salt (PPN$^+$)$_2${(X$^-$)$_2$Fe (TPyzPACl$_8$}·2C$_6$H$_4$Cl$_2$ (**2**) in the 260-1700 nm in KBr pellets.

and acetone free. FeTPyzPACl$_8$ (**1**) did not dissolve in *o*-dichlorobenzene and benzonitrile even upon heating. We dissolve compound **1** using the reaction of coordination of the CN$^-$ ligands by stirring of FeTPyzPACl$_8$ with 2.2 equivalents of bis(triphenylphosphoranylidene)ammonium cyanide (PPNCN) during 24 hours. Coordination of two CN$^-$ ligands to the iron(II) atoms of FeTPyzPACl$_8$ converts initially neutral compound to salt which is well soluble in pure *o*-dichlorobenzene in presence of two bulky PPN$^+$ cations. Crystals were precipitated by slow diffusion of hexane as black rhombs with size up to 0.5×0.4×0.1 mm and 22 % yield. Initially, the composition of the obtained salt was supposed to be (PPN$^+$)$_2${(CN$^-$)$_2$FeTPyzPACl$_8$}·2C$_6$H$_4$Cl$_2$ (**2**). However, wrong length of the C≡N and Fe-C(N≡C) bonds and the presence of additional electron density close to the C atom of the CN$^-$ groups allow one to suppose the presence of coordinated Cl$^-$ anions with low occupancy of only 0.130(8). There were no other halogens, for example Br$^-$, in the crystals of **2** according to the microprobe Energy Dispersive X-ray analysis. Thus, the exact composition of **2** was supposed to be (PPN$^+$)$_2${(CN$^-$)$_{1.74}$(Cl$^-$)$_{0.26}$FeTPyzPACl$_8$}·2C$_6$H$_4$Cl$_2$ (**2**) and in this case the lengths of the C≡N and Fe-C(N≡C) bonds are close to the published values (see Crystal structure section, Table 1). Most probably together with dicyanosubstituted (CN$^-$)$_2$FeTPyzPACl$_8$ dianion (the content of these dianions is 74 %) mixed (CN$^-$)(Cl$^-$) FeTPyzPACl$_8$ dianion is also formed (the content of these dianions is 26 %). The formation of mixed ligand complex is possible due to strong trans effect of cyanide ligands assisting substitution of one of two cyanides by additional ligands presented in the reaction mixture. Since reaction was carried out in *o*-dichlorobenzene, macrocycle contains chlorine atoms and some admixture of the Cl$^-$ anions can be in PPNCN salt ligand which substitutes cyanide can be only chlorine. There is a possibility for the presence of the (Cl$^-$)$_2$Fe^{III}TPyzPACl$_8$ monoanions admixture in the sample of **2** as well (about 13 %). However, in this case the occupancy of the PPN$^+$ cations position should be only 87 % (but experimentally we observed complete occupancy of the positions of these cations). Iron(III) and iron(II)

phthalocyanines also show different EPR spectra since iron(III) phthalocyanines are paramagnetic and manifest EPR signals, and iron(II) phthalocyanines are generally diamagnetic or contain even number of spins (S = 1, 2) and are not manifested in EPR. EPR silence of salt **2** supports the presence of only iron(II) species.

Optical Spectra

IR spectra of FeTPyzPACl$_8$ (**1**) and salt **2** are shown in Supporting information. The absorption bands of starting 1,2-dichloro-4,5-dicyanopyrazine (including characteristic bands at 2237 and 2250 cm^{-1} attributed to the C≡N vibrations) are absent in the spectrum of **1** showing no starting 1,2-dichloro-4,5-dicyanopyrazine in the sample of **1**. Instead of that, additional bands are observed in the spectrum of **1** at 1550-1690 cm^{-1}. These bands cannot be attributed to porphyrazine and most probably they are originate from acetylacetone and acetone which show intense absorption bands in this region due to the C=O vibrations. The formation of **2** is accompanied by the appearance of additional bands from the PPN$^+$ cations and solvent C$_6$H$_4$Cl$_2$ molecules (Supporting information). However, all absorption bands observed in the spectrum of **1** and attributed to the TPyzPACl$_8$ macrocycle are well reproduced in the spectrum of **2** but with a shift by 2-7 cm^{-1}. Thus the structure of macrocycle is retained at the conversation of **1** to **2**. The addition of the CN$^-$ ligands to the central iron(II) atoms of FeTPyzPACl$_8$ is manifested in the appearance of a well-resolved single band of the C≡N vibrations at 2103 cm^{-1} in the spectrum of **2**. It is seen that this band has intermediate position between those characteristic of the salts with the iron(II) and iron(III) complexes: 2085 cm^{-1} in the spectrum of (PPN$^+$)$_2$[(CN$^-$)FePc]·CH$_2$Cl$_2$[38] and 2088 cm^{-1} in the spectrum of (Bu$_4$N$^+$)$_2$[(CN$^-$)$_2$FeTAPPh$_8$], where TAP is tetraazaporphine and 2124 cm^{-1} in the spectrum of (Bu$_4$N$^+$)[(CN$^-$)$_2$Fe^{III}TAPPh$_8$].[39]

The UV-visible-NIR spectra of FeTPyzPACl$_8$ (**1**) and salt **2** are shown in Figure 1. The spectrum of FeTPyzPACl$_8$ (**1**) has the position of the *Q*- and Soret bands at 656, 475
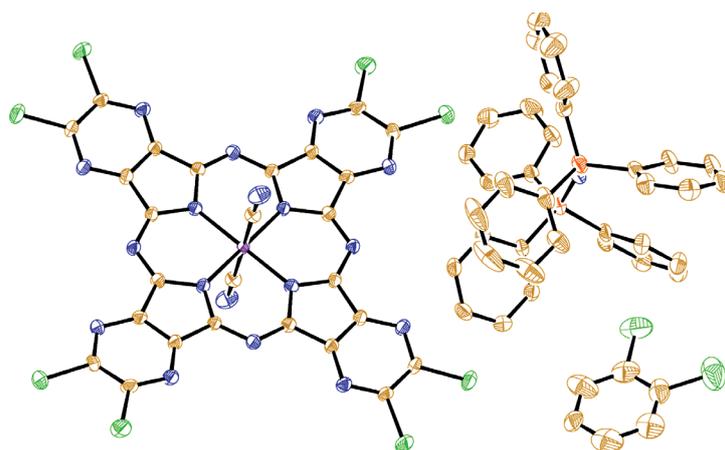
Figure 2. Components formed salt (PPN$^+$)$_2${(X$^-$)$_2$FeTPyzPACl$_8$}·2C$_6$H$_4$Cl$_2$ (**2**). Minor orientation of disordered C$_6$H$_4$Cl$_2$ molecule and the Cl$^-$ anions coordinated to the iron(II) atoms of FeTPyzPACl$_8$ and having low 13.0(8) % occupancy are not shown. Ellipsoid probability is 50 %.
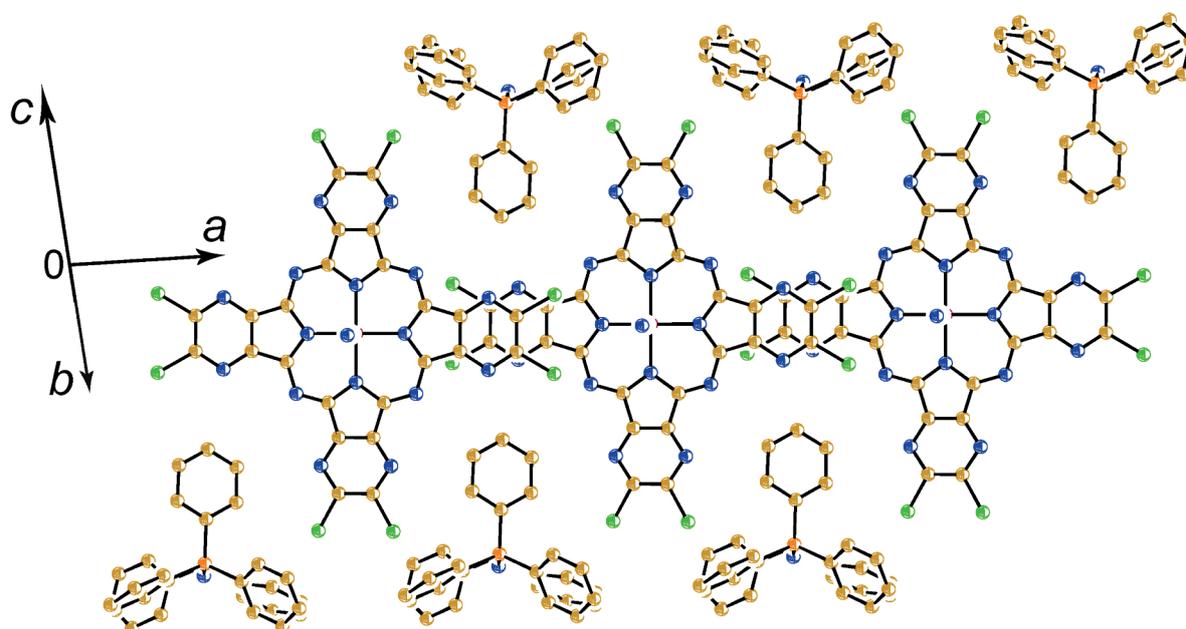

Figure 3. Crystal structure of **2**. View on the one-dimensional chains from the (X$^-$)$_2$FeTPyzPACl$_8$ dianions. Solvent C$_6$H$_4$Cl$_2$ molecules and the Cl$^-$ anions coordinated to the FeTPyzPACl$_8$ with 13.0(8) % occupancy are not shown for clarity.

and 327 nm. FeTAPPh$_8$ has the similar spectrum with the positions of the *Q*- and Soret bands at 626, 443 and 330 nm.[40] Addition of two axial anionic ligands to FeTPyzPACl$_8$ and spatial separation of porphyrazines by bulky PPN$^+$ cations produce spectrum with narrower absorption bands. Two bands in the spectrum of **2** at 657 and 326 nm have close position to those in the spectrum of **1** (656 and 327 nm). Whereas instead of broad band in the spectrum of **1** at 475 nm two intense bands at 550 nm and split band at 438 and 415 nm are appeared in the spectrum of **2**. These bands can be due to the addition of two CN$^-$ ligands to FeTPyzPACl$_8$ and manifestation of possible charge transfer transition from Fe to the CN$^-$ ligands (d$_\pi$-π*(CN$^-$)). Similar bands are observed in cyanide complex (Bu$_4$N$^+$)$_2$[(CN$^-$)$_2$FeTAPPh$_8$] at 451 and 575 nm in CH$_2$Cl$_2$ solution.[39]

Crystal Structure of 2

Salt **2** contains crystallographically independent half of (X$^-$)$_2$FeTPyzPACl$_8$ dianion, one PPN$^+$ cation and one solvent C$_6$H$_4$Cl$_2$ molecule (Figure 2). Solvent molecule is disordered between two orientations with the 0.482(3)/0.518(3) occupancies. Position of the ligand coordinated the iron(II) centers is occupied by the CN$^-$ and Cl$^-$ groups with 0.870(8)/0.130(8) occupancies, respectively.

The salt contains stepped one-dimensional chains from the (X$^-$)$_2$FeTPyzPACl$_8$ dianions arranged along the *a*-axis (Figure 3). As a result, dichloropyrazine fragments of neighboring (X$^-$)$_2$FeTPyzPACl$_8$ dianions are located one over another with nearly parallel arrangement and interplane distance of 3.459 Å. Several short van der Waals C, N, Cl(Prz)···C, N,

Cl(Prz) contacts are formed between them in the 3.49-3.65 Å range. The PPN⁺ cations are located in the vacancies arranged between pyrazine substituents of two (X⁻)$_2$FeTPyzPACl$_8$ dianions in such a way that one Ph$_3$P fragment is located above the TPryPACl$_8$ macrocycle and another Ph$_3$P fragment of PPN⁺ is located below this macrocycle. Each (X⁻)$_2$FeTPyzPACl$_8$ dianion is surrounded by eight PPN⁺ cations which form multiple C, H(PPN⁺)···C, N, Cl(TPyzPACl$_8$) contacts in the 3.30-3.46 and 2.70-2.90 Å ranges, respectively.

Molecular Structure of the (X⁻)$_2$FeTPrzPACl$_8$ Dianions

Geometric parameters of the (CN⁻)$_2$FeTPyzPACl$_8$ and (CN⁻)(Cl⁻)FeTPyzPACl$_8$ units are listed in Table 1. The accuracy for the determination of the C≡N, Fe-C(C≡N) and Fe-Cl bond lengths is rather low in **2** because of the disorder. Nevertheless, it is possible to conclude that the CN groups strongly coordinate to the iron(II) atoms of FeTPyzPACl$_8$ with short Fe-C bond whereas the Fe-Cl bond is noticeably longer in **2**. Close length of the Fe-C(C≡N) bonds is

observed in (PPN⁺)$_2$[(CN⁻)$_2$FePc]·CH$_2$Cl$_2$ (Table 1) with iron(II) phthalocyanine. It should be noted that the length of these bonds in negatively charged and partially oxidized (CN⁻)$_2$Fe^{III}Pc anions with the iron(III) phthalocyanine is noticeble longer (Table 1). The average length of the C≡N bonds in the cyanated iron(III) complexes is shorter than those in the cyanated iron(II) complexes (Table 1). Equatorial Fe-N bonds with the nitrogen atoms of the macrocycle is very close for (X⁻)$_2$FePc, (X⁻)$_2$Fe^{III}Pc and (X⁻)$_2$FeTPyzPACl$_8$ excepting compound [PTMA]$_x$[(CN⁻)$_2$Fe^{III}Pc]·y(CH$_3$CN) (See Table 1). Ligand-free FePc has slightly shorter average Fe-N(Pc) bonds of 1.926(1) Å.[17]

Only half of FeTPyzPACl$_8$ is crystallographically independent. Label of atoms, type of bonds and the displacement of atoms from the 24-atom PA plane are shown in Figure 4, bond length and average length of definite types of bonds in this macrocycle are listed in Table 2. The average length of the C-N bonds with the pyrrole and imine nitrogen atoms of 1.385(4) and 1.326(4) Å, respectively is very close to those determined for FePc of 1.382(2) and 1.324(2) Å, respectively.[19] Central porphyrazine macrocycle consisting of

Table 1. Molecular structures of the (X⁻)$_2$FePc dianions and (X⁻)$_2$Fe^{III}Pc monoanions in comparison with that of the (X⁻)$_2$FeTPyzPACl$_8$ dianions in **2** (X = CN⁻, Cl⁻).

Compound		The length of Fe-X bonds, Å	The length of C≡N bond, Å	The average length of Fe-N(Pc) bond, Å	Ref.
(PPN⁺)$_2$[(CN⁻)$_2$FePc]·CH$_2$Cl$_2$		1.960(6) (Fe-C)	1.171(7)	1.941(2)	[38]
(PPN⁺)[(CN⁻)$_2$Fe^{III}Pc]		1.976(4) (Fe-C)	1.151(5)	1.941(4)	[41]
(TPP⁺)[(CN⁻)$_2$Fe^{III}Pc]		1.981(2) (Fe-C)	1.142(2)	1.941(2)	[42]
[PTMA⁺]$_x$[(CN⁻)$_2$Fe^{III}Pc]·y(CH$_3$CN)					
	295 K	1.997(6) (Fe-C)	1.134(7)	1.927(3)	[43]
	123 K	1.995(5) (Fe-C)	1.148(6)	1.929(3)	
PXX[(CN⁻)$_2$Fe^{III}Pc]		1.984(3) (Fe-C)	1.147(3)	1.937(3)	[44]
(TPP⁺)[(Cl⁻)$_2$Fe^{III}Pc]$_2$		2.304(1) (Fe-Cl)	-	1.941(2)	[45]
(PPN⁺)[(Cl⁻)$_2$Fe^{III}Pc]$_2$		2.293(1) (Fe-Cl)	-	1.942(2)	[45]
(PPN⁺)$_2$[(CN⁻)$_2$FeTPyzPACl$_8$]	74 %	1.962(6) (Fe-C)	1.192(9)	1.941(3)	This
(PPN⁺)$_2$[(CN⁻)(Cl⁻)FeTPyzPACl$_8$]	26 %	2.410(12) (Fe-Cl)	-	1.941(3)	work

TPP: tetraphenylphosphonium cation; PTMA: phenyltrimethylammonium cation; PXX: perixanthenoxanthene.

Table 2. Bond length and average length of definite types of bonds in FeTPyzPACl$_8$ in **2**. Type of bonds are shown in Figure 4a.

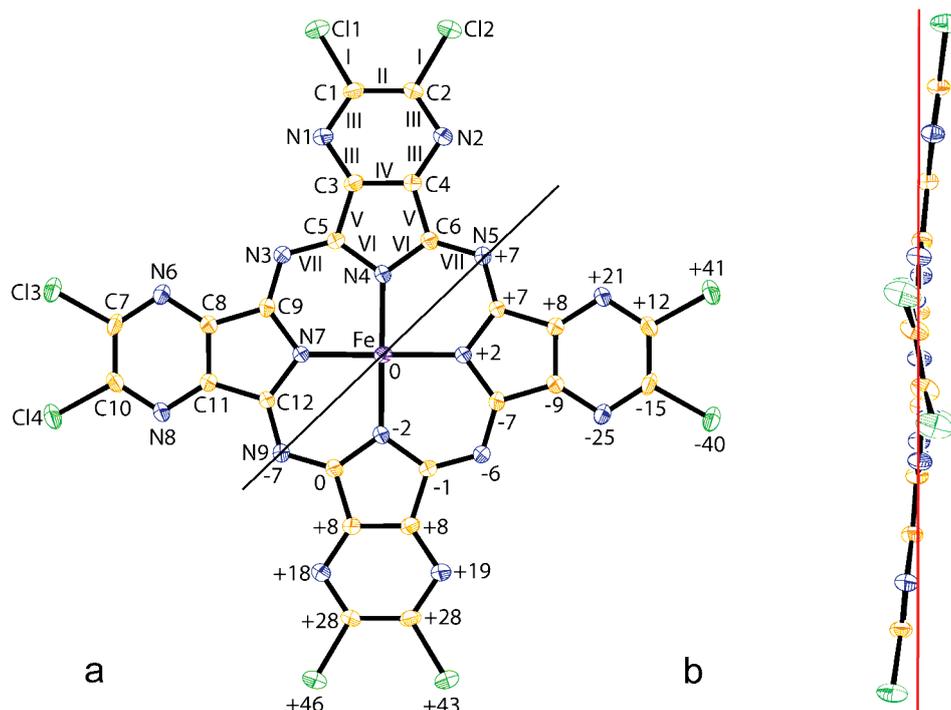| Type	Length, Å	Type	Length, Å	Type,	length, Å
Fe-N4	1.941(3)	C3-N	1.348(4)	Average length of C-C bonds of	
Fe-N7	1.941(3)	C4-N2	1.342(4)	type V is 1.455(4) Å	
Average length of Fe-N bonds is		C7-N6	1.338(4)	C5-N4	1.385(4)
1.941(3) Å		C8-N6	1.347(4)	C6-N4	1.385(4)
C1-Cl1	1.732(3)	C10-N8	1.321(4)	C9-N7	1.390(4)
C2-Cl2	1.728(3)	C11-N8	1.346(4)	C12-N7	1.378(4)
C7-Cl3	1.732(3)	Average length of C-N bonds of		Average length of C-N bonds of	
C10-Cl4	1.739(3)	type III is 1.336(4) Å		type VI is 1.385(4) Å	
Average length of C-Cl bonds of type I is		C3-C4	1.397(4)	C6-N5	1.327(4)
1.733(3) Å		C8-C11	1.398(4)	C5-N3	1.325(4)
C1-C2	1.420(4)	Average length of C-N bonds of type IV is		C9-N3	1.326(4)
C7-C10	1.411(4)	1.398(4) Å		C12-N9	1.325(4)
Average length of C-C bonds of		C3-C5	1.450(4)	Average length of C-N bonds of	
type II is 1.415(4) Å		C4-C6	1.456(4)	type VII is 1.326(4) Å	
C1-N1	1.331(4)	C8-C9	1.456(4)		
C2-N2	1.316(4)	C11-C12	1.457(4)		

Figure 4. Molecular structure of the centrosymmetric FeTPyzPACl$_8$ microcycle in the crystal of **2** (the coordinated CN$^-$ or Cl$^-$ ligands are not shown). (a) View perpendicular to the TPyzPACl$_8$ plane. Special symbols identifying each atom are shown in the upper left half of the diagram. In the lower right half of the Figure, perpendicular displacements of atoms relative to the mean 24-atom plane are shown in units of 0.01 Å. (b) View along the mean 24-atom plane which is shown by red line.

24 atoms is nearly planar with a weak displacement of atoms from the mean 24-atom plane. The iron(II) atoms are positioned exactly in this plane. However, the dichloropyrazine groups are strongly deviated from this plane. Two of four oppositely located groups are located above and below this plane with the displacement of the chlorine atoms by about 0.04 Å. Two other oppositely located groups are twisted relative to this plane in such a way that one chlorine atom is located above and one chlorine atom is located below this plane, both came out from the mean 24-atom plane by about 0.04 Å (see Figure 4a). Pyrazine groups are also slightly twisted relatively to the 24-atom PA plane in previously studied Co^{II}TPyzPAPy$_8$. However, in this case the displacements of N atoms of Prz from the 24-atom plane are smaller of 0.09-0.19 Å[30] than those in **2** (0.18-0.25 Å, Figure 4b).

Conclusions

The iron(II) octachlorotetrapyrazinoporphyrazine (FeTPrzPACl$_8$, **1**) was obtained from 1,2-dichloro-4,5-dicyanopyrazine and iron(II) acetylacetonate in 1-chloronaphthalene. FePyzPACl$_8$ was dissolved in *o*-dichlorobenzene by complex formation reaction with the CN$^-$ anions. The crystals of (PPN$^+$)$_2$\{(CN$^-$)$_{1.74}$(Cl$^-$)$_{0.26}$FeTPyzPACl$_8$\}·2C$_6$H$_4$Cl$_2$ (**2**) were obtained by diffusion of hexane. It is shown that the 24-atom porphyrazine macrocycle is nearly planar. However, the dichloropyrazine groups rather strongly displaced from the mean 24-atom plane. The (CN$^-$)$_2$FeTPyzPACl$_8$ dianions show similar geometry to those of the (CN$^-$)$_2$FePc dianions,

whereas the length of the Fe-C(C≡N) bonds in (CN$^-$)$_2$Fe^{III}Pc is noticeably longer. FeTPyzPACl$_8$ has strong absorption in the UV-visible range. Addition of axial anionic ligands increases the number of bands in the visible range. New bands appeared at 550, 438 and 415 nm can be attributed to possible charge transfer d$_\pi$-π*(CN$^-$) transition from Fe to the CN$^-$ ligands.

References

1. *Phthalocyanines: Properties and Applications* (Leznoff C.C., Lever A.B.P., Eds.), Cambridge, Wiley-VCH, **1989-1996**, Vols. 1-4.
2. *Handbook of Porphyrin Science: with Applications to Chemistry, Physics, Materials Science, Engineering, Biology and Medicine* (Kadish K.M., Smith M., Guilard R., Eds.), World Scientific, **2010**, Vol. 1.
3. Waltera M.G., Rudine AB., Wamser C.C. *J. Porphyrins Phthalocyanines* **2010**, *14*, 759-792.
4. Wöhrle D., Schnurpfeil G., Makarov S.G., Kazarin A., Suvorova O.N. *Macroheterocycles* **2012**, *5*, 191-202.
5. Kaliya O.L., Lukyanets E.A., Vorozhtsov G.N. *J. Porphyrins Phthalocyanines* **1999**, *3*, 592-610.
6. Ito O., D'Souza F. *Molecules* **2012**, *17*, 5816-5835.
7. Schramm C.S., Scaringe R.P., Stojakovic D.R., Hoffman B.M., Ibers J.A., Marks T.J. *J. Am. Chem. Soc*. **1980**, *102*, 6702-6713.
8. Inabe T., Tajima H. *Chem. Rev*. **2004**, *104*, 5503-5534.

Iron(II) Octachlorotetrapyrazinoporphyrazine Dianions

9. Miller J.S., Vazquez C., Calabrese J.C., McLean M.L., Epstein A.J. *Adv. Mater.* **1994**, *6*, 217-221.

10. Rittenberg D.K., Baars-Hibbe L., Böhm A.B., Miller J.S. *J. Mater. Chem.* **2000**, *10*, 241-244.

11. Tosatti E., Fabrizio M., Tóbik J., Santoro G.E. *Phys. Rev. Lett.* **2004**, *93*, 117002.

12. Konarev D.V., Zorina L.V., Khasanov S.S., Hakimova E.U., Lyubovskaya R.N. *New J. Chem.* **2012**, *36*, 48-51.

13. Tahiri M., Doppelt P., Fischer J., Weiss R. *Inorg. Chim. Acta* **1987**, *127*, L1-L3.

14. Hückstädt H., Homborg H. *Z. Anorg. Allg. Chem.* **1998**, *624*, 715-720.

15. Donzello M.P., Samuele C., Gustavo P., Claudio E. *Eur. J. Inorg. Chem.* **2009**, *12*, 1600-1607.

16. Konarev D.V., Zorina L.V., Khasanov S.S., Litvinov A.L., Otsuka A., Yamochi H., Saito G., Lyubovskaya R.N. *Dalton Trans.* **2013**, *42*, 6810-6816.

17. Konarev D.V., Kuzmin A.V., Simonov S.V., Khasanov S.S., Otsuka A., Yamochi H., Saito G., Lyubovskaya R.N. *Dalton Trans.* **2012**, *41*, 13841-13847.

18. Konarev D.V., Kuzmin A.V., Khasanov S.S., Lyubovskaya R.N. *Dalton Trans.* **2013**, *42*, 9870-9876.

19. Konarev D.V., Khasanov S.S., Ishikawa M., Otsuka A., Yamochi H., Saito G., Lyubovskaya R.N. *Inorg. Chem.* **2013**, *52*, 3851-3859.

20. Lever A.B.P., Milaeva E.P., Speier G. In: *Phthalocyanines, Properties and Applications* (Leznoff C.C., Lever A.B.P., Eds.), New York: Wiley-VCH, **1993**, *3*, 1-70 p.

21. Schlettwein D., Wöhrle D., Jaeger N.I. *Electrochem. Soc.* **1989**, *136*, 2882-2886.

22. Kobayashi N., Adachi K., Osa T. *Analytical Sciences* **1990**, *6*, 449-453.

23. Lebedeva T.A., Kulinich V.P., Shaposhnikov G.P., Efimova S.V., Korzhenevskii A.B., Koifman O.I. *Russ. J. Gen. Chem.* **2007**, *77*, 1944-1950.

24. Jang C.K., Kim S.H., Lee D.K., Jaung J.-Y. *Bull. Korean Chem. Soc.* **2008**, *29*, 1885-1886.

25. Taraymovich E.S., Enakieva Y.Y., Mitasova Y.V., Stuzhin P.A. *Macroheterocycles* **2010**, *3*, 48-50.

26. Kopecky K., Novakova V., Miletin M., Plistilova L., Berka P., Zimcik P. *Macroheterocycles* **2011**, *4*, 171-176.

27. Hill J.P., Subbaiyan N.K., D'Souza F., Xie Y., Sahu S., Sanchez-Ballester N.M., Richards G.J., Mori T., Ariga K. *Chem. Commun.* **2012**, *48*, 3951-3953.

28. Belozerova Y.I., Efimova S.V., Korzhenevskii A.B., Koifman O.I. *Russ. J. General Chem.* **2009**, *79*, 2678-2684.

29. Shishkin V.N., Kudrik E.V., Shaposhnikov G.P. *Russ. J. Coord. Chem.* **2005**, *31*, 516-520.

30. Donzello M.P., Ou Z., Dini D., Meneghetti M., Ercolani C., Kadish K.M. *Inorg. Chem.* **2004**, *43*, 8637-8648.

31. Bergami C., Donzello M.P., Ercolani C., Monacelli F., Kadish K.M., Rizzoli C. *Inorg. Chem.* **2005**, *44*, 9852-9861.

32. Manet I., Manoli F., Donzello M.P., Ercolani C., Vittori D., Cellai L., Masi A., Monti S. *Inorg. Chem.* **2011**, *50*, 7403-7411.

33. Donzello M.P., Viola E., Ercolani C., Fu Z., Futur D., Kadish K.M. *Inorg. Chem.* **2012**, *51*, 12548-12559.

34. Zimcik P., Novakova V., Miletin M., Kopecky K. *Macroheterocycles* **2008**, *1*, 21-28.

35. Lekitima J.N., Ozoemena K.I., Jafta C.J., Kobayashi N., Song Y., Tong D., Chen S., Oyama M. *J. Mater. Chem. A* **2013**, *1*, 2821-2826.

36. Bruker Analytical X-ray Systems, Madison, Wisconsin, U.S.A, **1999**.

37. Sheldrick G.M., SHELX97, University of Göttingen, Germany, **1997**.

38. Köppers H., Eulert H.-H., Hesse K.-F., Kalz W., Homborg H. *Z. Naturforsch.* **1986**, *B41*, 44-47.

39. Stuzhin P.A. *Russ. J. Coord. Chem.* **1995**, 21, 117-123.

40. Stuzhin P.A. *Macroheterocycles* **2009**, *2*, 114-129.

41. Köppers H., Kalz W., Homborg H. *Acta Cryst. C* **1985**, *41*, 1420-1423.

42. Matsuda M., Naito T., Inabe T., Hanasaki N., Tajima H., Otsuka T., Awaga K., Narymbetov B., Kobayashi H. *J. Mater. Chem.* **2000**, *10*, 631-636.

43. Matsuda M., Naito T., Inabe T, Hanasaki N., Tajima H. *J. Mater. Chem.* **2001**, *11*, 2493-2497.

44. Matsuda M., Asari T., Naito T., Inabe T., Hanasaki N., Tajima H. *Bull. Chem. Soc. Jpn.* **2003**, *76*, 1935-1940.

45. Yu D.E.C., Matsuda M., Tajima H., Kikuchi A., Taketsugu T., Hanasaki N., Naito T., Inabe T. *J. Mater. Chem.* **2009**, *19*, 718-723.